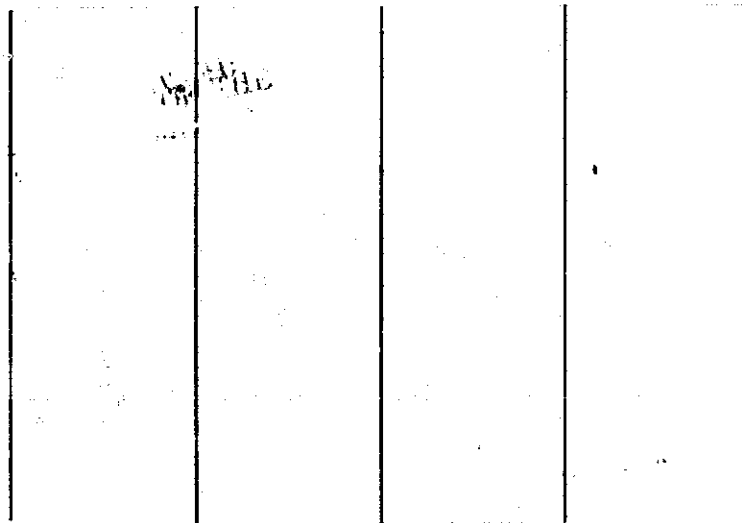# General Disclaimer

One or more of the Following Statements may affect this Document
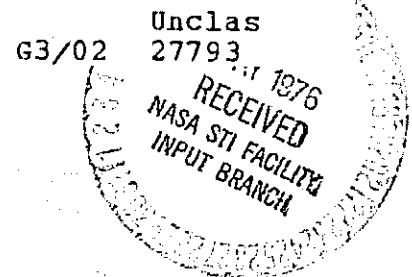
- This document has been reproduced from the best copy furnished by the organizational source. It is being released in the interest of making available as much information as possible.

- This document may contain data, which exceeds the sheet parameters. It was furnished in this condition by the organizational source and is the best copy available.

- This document may contain tone-on-tone or color graphs, charts and/or pictures, which have been reproduced in black and white.

- This document is paginated as submitted by the original source.

- Portions of this document are not fully legible due to the historical nature of some of the material. However, it is the best reproduction available from the original submission.

Princeton University

DEI SUB NUMINE VIGET

Department of
Aerospace and
Mechanical Sciences

STEADY INCOMPRESSIBLE

VARIABLE THICKNESS SHEAR LAYER AERODYNAMICS

by

M. R. Chi[*]

AMS Report No. 1259

January 1976

*Assistant-in-Research, Department of Aerospace and Mechanical Sciences,
Princeton University, Princeton, New Jersey.

TABLE OF CONTENTS

ABSTRACT

A shear flow aerodynamic theory for steady incompressible flows
is presented for both the lifting and non-lifting problems. The unique
feature of the present theory is the consideration of the slow variation
of the boundary layer thickness. The slowly varying behavior is treated
by using the method of multi-time scales. The analysis begins with
the elementary wavy wall problem and, through Fourier superpositions
over the wave number space, the shear flow equivalents to the aero-
dynamic transfer functions of classical potential flow are obtained.
The aerodynamic transfer functions provide integral equations which
relate the wall pressure and the upwash. Computational results are
presented for the pressure distribution, the lift coefficient, and
the center of pressure travel along a two dimensional flat plate in a
shear flow. The aerodynamic load is decreased by the shear layer,
compared to the potential flow, while the variable thickness shear
layer decreases it less than the uniform thickness shear layer based
upon equal maximum shear layer thicknesses.

- ii -

NOMENCLATURE

a	- perturbed characteristic length in mean flow direction
A, A_0, A_1	- Aerodynamic influence functions in physical space
$\bar{A}$, A_0^*, A_1^*	- Aerodynamic influence functions in wave number space
A_ν	- See Equation (16)
b	- Wing span
c	- Wing chord
$f(x,y)$	- Surface Contour (Figure 1)
$\bar{f}$	- Wavy wall amplitude
$I_\nu(\ )$	- Bessel function of second kind of order ν
K, K_A, K_B	- Aerodynamic kernel functions in physical space
$\bar{K}$, K_A^*, K_B^*	- Aerodynamic kernel functions in wave number space
ℓ	- Characteristic length in mean flow direction
L, L_1	- See Equations (16) and (21)
N	- Exponent in shear layer velocity profile (see Eq.(4)).
$p(x,y)$	- Fluid perturbation pressure
$\bar{p}$	- Wavy wall fluid pressure
$p_w(x,y)$, p_{w0}, p_{w1}	- Wall pressure
$\bar{p}_w$	- Wavy wall fluid pressure at wall
R	- $\equiv (\alpha^2 + \gamma^2)^{1/2}$
$\bar{R}$	- $\equiv R\delta$
u, v, w	- Fluid perturbation velocities in x, y and z directions
U	- Shear flow mean velocity
U_1	- Free stream velocity
$W(x,y)$	- Upwash $\equiv U_1\frac{\partial f(x,y)}{\partial x}$
$W^*(x,y)$	- Wavy wall upwash
W_{eq}	- See Equation (40)

x, y, z - Coordinate axes

x', y', z' - (see Figure 1)

ξ, η, ζ - See Equation (8)

∇^2 $- \equiv \dfrac{\partial^2}{\partial x^2} \quad \dfrac{\partial^2}{\partial y^2} \quad \dfrac{\partial^2}{\partial z^2}$

ρ - Fluid density

Γ - Gamma function

$\delta, \delta(x,y)$ - Boundary layer thickness

δ_{max} - Maximum boundary layer thickness along chord (trailing edge)

α, γ - Wave numbers in x and y directions

$\bar{\alpha}, \bar{\gamma}$ $- \bar{\alpha} \equiv \alpha\, \delta_{max}, \; \bar{\gamma} = \gamma\, \delta_{max}$

ε $- \equiv \delta_{max}/\ell \;$ or $\; \delta_{max}/c$

ε' $- \equiv \delta_{max}/b$

ν $- \equiv \dfrac{1}{2} + \dfrac{1}{N}\;$ in main text

     - fluid kinematic viscosity in appendix.

C_L $- \equiv$ total lift $/ \left(\dfrac{1}{2}\, \rho\, U^2.c \right)$

C_M $- \equiv$ moment about leading edge $/ \left(\dfrac{1}{2} \rho\, U^2 . c^2 \right)$

I. INTRODUCTION

To account for the presence of the boundary layer adjacent to any solid surface in a fluid flow theoretical analyses of the shear flow effect have been made by many researchers [1-20]. Common to all the above analyses is the assumption of the uniform thickness of the boundary layer initially present before the solid boundary surface is deformed. However, the boundary layer normally grows in the mean flow direction and one naturally would like to know how the boundary layer thickness variation affects the aerodynamic load on the solid surface. This paper deals with this problem but is restricted to the steady, incompressible flow with a slowly varying boundary layer. Similar reasoning can be extended to unsteady and compressible flows.

Since this report is an extension of Ventres' work [19], we first briefly review and quote his uniform thickness results and then develop a theory for the slowly varying boundary layer problem.

II. BRIEF REVIEW OF VENTRES' RESULTS

Consider a steady, incompressible shear flow over a surface whose deflection is given as $z = f(x,y)$. See Figure 1. The surface deflection produces a small disturbance from an initially parallell shear flow $u = U(z)$, $v = w = 0$. The function $U(z)$ is constant for $z > \delta$ so that the shear layer is limited to the region $0 < z < \delta$ adjacent to the surface.

With the choice of the mean flow $U(z) = U_1 U_\infty (z/\delta)^{1/N}$ Ventres was able to relate semi-analytically the upwash $W(x,y)$ everywhere in the $z = 0$ plane to the perturbation pressure distribution on the wing $p(x,y)$ (recall that we are dealing with the lifting problem) according to

$$\frac{W(x,y)}{U_1} = \iint_{wing} K(x-\xi,\ y-\eta)\ \frac{p(\xi,\eta)}{\rho U_\infty^2}d\xi d\eta$$

where $\dfrac{W(x,y)}{U_1} \equiv \dfrac{\partial f}{\partial x}(x,y)$ and $f(x,y)$ is the wall deflection. The

two-dimensional kernel function $K(x)$, which is of fundamental importance, is shown in Figure 2 for $N = 7$ and 11. Also shown is the potential flow result,

$$K(x) = \frac{1}{\pi x}$$

which is labelled in the Figure as $N = \infty$. All three curves have a common asymptote as $x/\delta \to \infty$, and in fact are essentially identical for $x/\delta > 2$ or so. Since K physically is the upwash caused by an impulse pressure, this implies that the influence region of the shear layer is limited to a distance on each side of the source point comparable to the shear layer

thickness, or the shear layer effect is "nearly local". This points up the possibility of accounting approximately for the effect of slowly varying boundary layer thickness by inserting a variable $\delta(x)$ directly into Ventres uniform thickness shear layer theory. The problem is then how to insert the variable $\delta(x)$ appropriately. The rost of this paper will demonstrate the reasonable way of doing it using the multi-time scale concept [21].

III.   SHEAR FLOW WITH SLOWLY VARYING BOUNDARY LAYER THICKNESS

(a) Governing Equations And Boundary Conditions

Detailed order of magnitude analysis given in the Appendix shows that the perturbation pressure $p(x,y,z)$ satifies

$$\nabla^2 p - 2 \frac{\frac{\partial U}{\partial z}}{U} \frac{\partial p}{\partial z} = 0 \tag{1}$$

The associated boundary conditions are [12, 19]

$$\left. \frac{\partial p}{\partial z} \right|_{z=z_0} = -\rho U \, (z = z_0) \, \frac{\partial w}{\partial x} \tag{2}$$

on the solid surface as $z_0 \to 0$, where

$$w \left. \right|_{z=z_0} = U \left. \right|_{z=z_0} \cdot \frac{\partial f}{\partial x}$$

and the finiteness condition

$$p \to 0 \quad \text{as} \quad z \to \infty \tag{3}$$

We assume the mean flow,

$$U = \begin{cases} U_1 & z \geq \delta(x,y) \\ U_1 \left[\frac{z}{\delta(x,y)} \right]^{1/N} & z \leq \delta(x,y) \end{cases} \tag{4}$$

While assuming a discontinuity in the mean flow velocity gradient across $z = \delta(x,y)$, we impose the continuity of the pressure and the pressure gradient

- 5 -

across the boundary layer edge, i.e.

at $z = \delta(x,y)$

$$p(x,y,z = \delta^-(x,y)) = p(x,y,z = \delta^+(x,y))$$

and $\frac{\partial p}{\partial z} (x,y,z = \delta^-(x,y)) = \frac{\partial p}{\partial z}(x,y,z = \delta^+(x,y))$ \hfill (5)

From Equations(1) and (4) the pressure within the shear layer
region satisfies

$$\nabla^2 p - \frac{2}{Nz} \frac{\partial p}{\partial z} = 0 \hfill (6)$$

which will be solved along with the wall boundary condition,
Equation (2), i.e.

$$\left. \frac{\partial p}{\partial z} \right|_{z=z_0} = - \rho \, U^2 \, (z=z_0) \, \frac{\partial^2 f}{\partial x^2} \qquad \text{as } z_0 \to 0 \hfill (7)$$

and another boundary condition at the boundary layer edge to be derived
from the field equation outside the boundary layer satisfying the
finiteness condition far away from the solid surface (see Equation (14)).

(b) Normalization

In view of the slowly varying behavior it is convenient to write
the boundary layer thickness

$$\delta = \delta \, (\varepsilon\xi, \, \varepsilon'\eta)$$

where $\varepsilon \ll 1$ and $\varepsilon' \ll 1$. Here, ε and ε' are non-dimensional para-
meters characterizing the slow variation of the boundary layer thickness

REPRODUCIBILITY OF THE
ORIGINAL PAGE IS POOR

in the x and y directions respectively, e.g. $\varepsilon = \delta_{max}/_{\ell}$ and $\varepsilon' = \delta_{max}/_{b}$. δ_{max} is the trailing edge shear layer thickness which is usually the maximum along the chord of an airfoil and b is the wing span. ξ and η are non-dimensional coordinates defined as

$$\xi \equiv \frac{x}{\delta_{max}} \quad , \quad \eta = \frac{y}{\delta_{max}} \quad , \quad \zeta = \frac{z}{\delta(\varepsilon\xi, \varepsilon'\eta)} \tag{8}$$

The definition for ζ has the advantage that all boundary conditions are applied on constant values of ζ, e.g. $\zeta = 0$, $= 1$ and $\rightarrow \infty$ (corresponding to $z = 0$, $\delta(x,y)$, and $\rightarrow \infty$).

(c) Wavy Wall Problem - Elementary Solution

Consider a wavy wall whose profile is described by the real part of the complex function

$$f(x,y) = \bar{f} \, e^{\,i(\alpha x + \gamma y)}$$
$$= \bar{f} \, e^{\,i(\bar{\alpha}\xi + \bar{\gamma}\eta)} \tag{9}$$

where $\bar{\alpha} = \alpha \, \delta_{max}$, $\bar{\gamma} = \gamma \, \delta_{max}$.
The wavy wall will generate a perturbation pressure field of the following form.

$$p = \bar{p}(\zeta, \varepsilon\xi, \varepsilon'\eta; \bar{\alpha}, \bar{\gamma}; \varepsilon, \varepsilon') \, e^{\,i(\bar{\alpha}\xi + \bar{\gamma}\eta)} \tag{10}$$

in which the slight amplitude modulation due to the slow boundary layer variation is manifested by the functional dependence of $\bar{p}$ on $\varepsilon\xi, \varepsilon'\eta$ ε and ε'. We further assume the following series expansion for $\bar{p}$ since $\varepsilon \ll 1$ and $\varepsilon' \ll 1$[21].

$$\overline{p}(\zeta, \epsilon\xi, \epsilon'\eta; \overline{\alpha}; \overline{\gamma}; \epsilon, \epsilon') = \overline{p}_0(\zeta, \epsilon\xi, \epsilon'\eta; \overline{\alpha}, \overline{\gamma})$$

$$+ \epsilon\overline{p}_1(\zeta, \epsilon\xi, \epsilon'\eta; \overline{\alpha}, \overline{\gamma}) \qquad (11)$$

$$+ \epsilon'\overline{p}_1'(\zeta, \epsilon\xi, \epsilon\eta; \overline{\alpha}, \overline{\gamma}) + \text{H.O.T.}$$

Rewriting Equation (6) in terms of ξ, η, ζ rather than x, y, z by means of Equation (8) and substituting the assumed wavy wall pressure solution, Equations (10) and (11), into the resultant equation, one can show that the lowest order governing equation for $\overline{p}_0$ is

$$\frac{\partial \overline{p}_0}{\partial \zeta^2} - \frac{2}{N\zeta} \frac{\partial \overline{p}_0}{\partial \zeta} - \left[\left(\frac{\delta}{\delta_{max}} \right)^2 \overline{R}^2 \right] \overline{p}_0 = 0 \qquad (12)$$

where δ is the variable boundary layer thickness. The higher order equations, which are not shown here, have lower order solutions as their forcing functions.

The required wall boundary condition for solving Equation (12) is obtained by substituting Equations (9) and (10) and (11) into Equation (7) and identifying the zeroth order relation, namely

$$\left. \frac{\partial \overline{p}_0}{\partial \zeta} \right|_{z=z_0} = \rho \left(\overline{\alpha} \frac{\delta}{\delta_{max}} \right)^2 U^2 \left(\frac{z_0}{\delta} = \zeta_0 \right) \left(\frac{\delta_{max}}{\delta} \frac{\overline{z}}{\delta_{max}} \right) \qquad (13)$$

as $\zeta_0 \to 0$. The higher order wall boundary conditions are trivial,

$$\left. \frac{\partial \overline{p}_i}{\partial \zeta} \right|_{\zeta=\zeta_0} = 0 \quad \text{for all} \quad i \geq 1 . \quad \text{as} \quad \zeta_0 \to 0$$

Another boundary condition at the edge of the shear layer for solving Equation (12) is obtained by setting $N = \infty$ in Equation (12) and applying

the finiteness condition as $\zeta \to \infty$, i.e.

$$\frac{\partial \bar{P}_0}{\partial \zeta} + \left(\frac{\delta \cdot \bar{R}}{\zeta_{max}}\right) \bar{P}_0 = 0 \tag{14}$$

Everywhere outside the boundary layer and in particular at the boundary layer edge $\zeta = 1$ because of the continuity of the pressure and the pressure gradient across $\zeta = 1$.

Equation (12) subject to boundary conditions (13) and (14) gives the wall pressure solution [19],

$$\frac{\bar{P}_W}{\rho U_1^2}(\alpha,\gamma,\delta(x,y)) = \bar{A}(\alpha,\gamma,\delta(x,y)) \frac{W*}{U_1}(\alpha,\gamma)\left(\frac{1}{2\pi}\right)^2 \tag{15}$$

where
$$\bar{A} = \frac{i}{A_\nu} \frac{\alpha}{R} \left(\frac{2}{R\delta}\right)^{2/N} \cdot L(R\delta)$$

$$A_\nu = \frac{\nu\Gamma(1-\nu)}{\Gamma(1+\nu)}$$

$$L(R\delta) = \frac{I_\nu(R\delta)+I_{\nu-1}(R\delta)}{I_{-\nu}(R\delta)+I_{1-\nu}(R\delta)} \tag{16}$$

$$\frac{W*}{U_1}(\alpha,\gamma) = i \alpha \bar{F} \cdot (2\pi)^2$$

The solution is the same as Ventres' except his uniform thickness has been replaced by the variable thickness $\delta(x,y)$. Henceforward, the 0 subscript on p_{w_0} is dropped, for simplicity.

Thus we have obtained the pressure amplitude function for the wavy wall problem using the shear flow model of slowly varying boundary layer. The pressure amplitude is proportional to the upwash $\dfrac{W^*}{\overline{U}_1}$ as expected in a linear theory.

For an arbitrary wall deflection we can use the superposition property of a linear theory to form Fourier integrals. However the Fourier superposition should be performed carefully as shown in the following two sections.

(d) Pressure Load for an Arbitrary Wall Deflection - Non-lifting Problem

We have just derived the linear relation for wall pressure amplitude (15) for a wavy wall problem. Through the linear superposition of the wavy wall solutions over all possible wave numbers, the wall pressure due to any properly behaved wall deflection is

$$\frac{P_W}{\rho \overline{U}_1^2}(x,y,\delta(x,y)) = \int\int_{-\infty-\infty}^{\infty\ \infty} \frac{\overline{P}_W}{\rho \overline{U}_1^2}(\alpha,\gamma;\delta(x,y)) \, e^{i(\alpha x+\gamma y)} \, d\alpha d\gamma \qquad (17)$$

Substitution of Equation (15) into Equation (17) yields

$$\frac{P_W}{\rho \overline{U}_1^2}(x,y,\delta(x,y)) = \left(\frac{1}{2\pi}\right)^2 \int\int_{-\infty}^{\infty} \overline{A}(\alpha,\gamma;\delta(x,y)) \, \frac{W^*}{\overline{U}_1}(\alpha,\gamma) \, e^{i(\alpha x+\gamma y)} d\alpha d\gamma \qquad (18)$$

To write Equation (18) as an integral in physical space, we define

$$A(x',y',\delta(x,y)) \equiv \left(\frac{1}{2\pi}\right)^2 \iint_{-\infty}^{\infty} \overline{A}(\alpha,\gamma;\delta(x,y))\, e^{-i(\alpha x'+\gamma y')}\, d\alpha d\gamma \qquad (18a)$$

which implies

$$\overline{A}(\alpha,\gamma;\delta(x,y)) = \iint_{-\infty}^{\infty} A(x',y';\delta(x,y))\, e^{i(\alpha x'+\gamma y')}\, dx'dy' \qquad (18b)$$

In addition, we have

$$\frac{W}{\overline{U}_1}(x,y) = \left(\frac{1}{2\pi}\right)^2 \iint_{-\infty}^{\infty} \frac{W*}{\overline{U}_1}(\alpha,\gamma)\, e^{-i(\alpha x+\gamma y)}\, d\alpha d\gamma \qquad (18c)$$

Using (18a) and (18c), one can easily show that Equation (18) is equivalent to

$$\frac{P_w}{\rho \overline{U}_1^2}(x,y,\delta(x,y)) = \iint_{-\infty}^{\infty} A(x-x',\, y-y';\delta(x,y))\, \frac{W}{\overline{U}_1}(x',y')\, dx'dy' \qquad (19)$$

Alternatively, one can arrive at Equation (19) by using the Fourier convolution theorem directly from Equation (18) with the recognition that Equation (18a) is a definition af $A(x',y';\, \delta(x,y))$ in terms of $\overline{A}(\alpha,\gamma;\delta(x,y))$ and $\delta(x,y)$ is treated as irrelevant to the Fourier integrals.

Either of Equation (18) and Equation (19) can be used to calculate the wall perturbation pressure for a given upwash $W(x,y)$. However, a drastic reduction of computation time can be made by recognizing that the quantity $(1 - \frac{\delta(x,y)}{\delta_{max}})$ is everywhere smaller than one except near the leading edge where $\delta(x,y) \to 0$. Hence, we can expand the function $\overline{A}$ in Equation (18) in terms of a power series of $(1 - \frac{\delta(x,y)}{\delta_{max}})$; the resultant pressure solution presumably will be valid everywhere except

near the leading edge where our theory is not expected to be accurate in any event because of the rapidly changing boundary layer thickness. It can be shown that

$$\bar{A} = A_0^* + \left(1 - \frac{\delta(x,y)}{\delta_{max}}\right)A_1^* + 0\left(1 - \frac{\delta(x,y)}{\delta_{max}}\right)^2 \tag{20}$$

where

$$A_0^* = \frac{1}{\bar{A}_\nu}\frac{\alpha}{R}\left(\frac{2}{R\delta_{max}}\right)^{2/N} L\left(R\delta_{max}\right)$$

$$A_1^* = \frac{1}{\bar{A}_\nu}\frac{\alpha}{R}\left(\frac{2}{R\delta_{max}}\right)^{2/N} \left[\frac{2}{N} L(R\delta_{max}) - L_1(R\delta_{max})\right]$$

$$L(R\delta_{max}) = \frac{I_\nu(R\delta_{max}) + I_{\nu-1}(R\delta_{max})}{I_{-\nu}(R\delta_{max}) + I_{1-\nu}(R\delta_{max})} \tag{21}$$

$$L_1(R\delta_{max}) = \frac{4\cos\pi/N}{N\pi R\delta_{max}} \Bigg/ \left[I_\nu(R\delta_{max}) + I_{-\nu}(R\delta_{max})\right]^2$$

Substitution of Equation (20) into Equation (18) and the use of the Fourier convolution theorem gives the wall pressure,

$$\frac{P_w}{\rho U_1^2}(x,y) = \frac{P_{w0}}{\rho U_1^2} + \left(1 - \frac{\delta(x,y)}{\delta_{max}}\right)\frac{P_{w1}}{\rho U_1^2}(x,y) + 0\left(1 - \frac{\delta(x,y)}{\delta_{max}}\right)^2 \tag{22}$$

where

$$\frac{P_{w0}}{\rho U_1^2}(x,y) = \int\int_{-\infty}^{\infty} A_0(x-x', y-y', \frac{W(x',y')}{U_1}) \, dx'dy' \tag{23}$$

and

$$\frac{P_{W_1}(x,y)}{\rho U_1^2} = \int\!\!\int_{-\infty}^{\infty} A_1(x-x',y-y')\, \frac{W}{U_1}(x',y')\,dx'dy'$$

A_0 and A_1 are the Fourier inversion of A_0^* and A_1^* defined in Equation (21) and can be evaluated numerically, i.e.

$$A_0(x,y) = \left(\frac{1}{2\pi}\right)^2 \int\!\!\int_{-\infty}^{\infty} A_0^*\, e^{\,i(\alpha x+\gamma y)}\,d\alpha d\gamma$$

$$A_1(x,y) = \left(\frac{1}{2\pi}\right)^2 \int\!\!\int_{-\infty}^{\infty} A_1^*\, e^{\,i(\alpha x+\gamma y)}\,d\alpha d\gamma$$

Here, A_0 is the same as Ventres' result except his uniform thickness has been replaced by the maximum thickness δ_{max}. A_1 is a new function used to calculate the pressure correction due to the slowly variation of the boundary layer, but it is independent of the detailed variation of the boundary layer which enters the pressure solution in the factor $(1-\frac{\delta(x,y)}{\delta_{max}})$ in Equation (22). One can show that A_1 vanishes as δ_{max} approaches zero, a natural result because of the loss of the "variation" of the boundary layer as the boundary layer vanishes.

Thus we have derived a scheme for calculating the pressure load on any solid surface which is deformed slightly from its flat position and exposed to a shear flow whose boundary layer thickness slowly varies. In aeronautical jargon, we have solved the non-lifting problem because the equations we have found (Equations (19) and (23)) require the upwash $W(x,y)$ being given everywhere in the $z = 0$ plane. For the technologically more important lifting problem the above Fourier superposition of the pressure load alone is not sufficient and a slightly

different procedure is needed as will be seen in the next section.

(e) The Pressure Load for an Arbitrary Wall Deflection - Lifting Problem

For the lifting problem, it is convenient to write Equation (15) as

$$\left(\frac{1}{2\pi}\right)^2 \frac{W^*}{U_1} = \overline{K} \frac{\overline{p}_w}{\rho U_1^{\,2}} (\alpha,\gamma;\delta(x,y)) \qquad (24)$$

where $\overline{K}$ is the reciprocal of $\overline{A}$ defined in Equation (16) and is the same as
Ventres' kernel with his uniform thickness replaced by the variable
$\delta(x,y)$, i.e.

$$\overline{K} = \frac{A_v}{i} \frac{R}{\alpha} \left(\frac{R\delta}{2}\right)^{2}\!\Big/ N\!\Big/ L(R\delta) \qquad (25)$$

Multiplied by $e^{i(\alpha x+\gamma y)}$ and integrated over (α,γ) space, Equation (24)
results in the following upwash equation.

$$\frac{W}{U_1}(x,y) = \left(\frac{1}{2\pi}\right)^2 \iint \frac{W^*}{U_1} e^{i(\alpha x+\gamma y)} d\alpha d\gamma \qquad (26)$$

$$= \iint \overline{K}(\alpha,\gamma;\delta(x,y)) \frac{\overline{p}_w(\alpha,\gamma;\delta(x,y))}{\rho U_1^{\,2}} e^{i(\alpha x+\gamma y)} d\alpha d\gamma$$

In addition, the superposition result Equation (17) still holds for
the lifting problem, i. e.

$$\frac{p_w}{\rho U_1^{\,2}}(x,y;\delta(x,y)) = \int\!\!\int_{-\infty}^{\infty} \frac{\overline{p}_w}{\rho U_1^{\,2}}(\alpha,\gamma;\delta(x,y)) e^{i(\alpha x+\gamma y)} d\alpha d\gamma \qquad (27)$$

which can be formally inverted to give

$$\bar{p}_w(\alpha,\gamma;\delta(x,y)) = \left(\frac{1}{2\pi}\right)^2 \iint \frac{p_w}{\overline{\rho U}_1^2}(x',y';\delta(x,y)) \, e^{-i(\alpha x'+\gamma y')}dx'dy' \qquad (28)$$

In obtaining Equation (28), $\delta(x,y)$ has been treated as irrelevant to the integral operation. Note that $p_w(x',y';\delta(x,y))$ is not the real wall pressure as it should have been if x', y' are replaced by x, y. Substituion of Equation (28) into Equation (26) gives the familiar kernel function form for the lifting problem.

$$\frac{w}{\overline{U}_1}(x,y) = \iint_{wing} K(x-x', y-y';\delta(x,y)) \frac{p_w}{\overline{\rho U}_1^2}(x',y';\delta(x,y)) \, dx'dy' \qquad (29)$$

where
$$K(x,y,\delta(x,y)) \equiv \left(\frac{1}{2\pi}\right)^2 \iint_{-\infty}^{\infty} \bar{K}(\alpha,\gamma;\delta(x,y)) e^{-i(\alpha x+\gamma y)} d\alpha d\gamma \qquad (30)$$

The domain of integration in Equation (29) is within the wing surface area because $p_w = 0$ everywhere off the wing for the lifting problem. The kernel function inversion, Equation (30), can be evaluated semi-analytically according to Ventres [19]. A convenient splitting of $\bar{K}$ into two parts is

$$\bar{K} = \bar{K}_1 + \bar{K}_2 \qquad (31)$$

where

$$\bar{K}_1 = \frac{A_\nu}{i} \frac{R}{\alpha} \left(\frac{R\delta}{2}\right)^{2/N} \left(\frac{1}{L(R\delta)} - 1\right)$$

$$\overline{K}_2 = \frac{A_\nu}{I} \frac{R}{\alpha} \left(\frac{R\delta}{2}\right)^{2/N}$$

$$A_\nu = \frac{\nu\Gamma(1-\nu)}{\Gamma(1+\nu)}$$

$\overline{K}_1$ can be inverted numerically to give K_1 and $\overline{K}_2$ can be inverted analytically to give K_2 so that

$$K = K_1 + K_2 \tag{32}$$

For two dimensional shear flow,

$$K_2(x,\delta(x)) = \frac{A_\nu}{\pi x} \left(\frac{\delta}{2|x|}\right)^{2/N} \Gamma(2\nu)\cos\left(\frac{\pi}{N}\right),$$

and for three dimensional flow

$$K_2(x,y,\delta(x,y)) = - \frac{2\nu^2\delta^{2/N}}{\pi} \int_{-\infty}^{x} \frac{U \, dU}{(\sqrt{U^2+y^2})^{3+2/N}}$$

Similar to the non-lifting problem an expansion of the tranformed kernel $\overline{K}$ in terms of the quantity $\left(1 - \frac{\delta(x,y)}{\delta_{max}}\right)$ can be made.

$$\overline{K} = K_A^* + \left(1-\frac{\delta(x,y)}{\delta_{max}}\right) K_B^* + 0 \left(1-\frac{\delta(x,y)}{\delta_{max}}\right) \tag{33}$$

where

$$K_A^* = \frac{A_\nu}{I} \frac{R}{\alpha} \left(\frac{R\delta_{max}}{2}\right)^{2/N} \Big/ L \left(R\delta_{max}\right) \tag{34}$$

$$K_B^* = \frac{A_\nu}{\frac{1}{L}} \frac{R}{\alpha} \left(R\frac{\delta_{max}}{2}\right)^{2/N} \left(\frac{L_1(R\delta_{max})}{L(R\delta_{max})} - \frac{2}{N}\right) \Big/ L(R\delta_{max})$$

Substitution of Equation (33) into Equation (30) gives

$$K(x,y,\ (x,y)) = K_A(x,y) + \left(\frac{1-\delta(x,y)}{\delta_{max}}\right) K_B(x,y) + 0\left(1-\frac{\delta(x,y)}{\delta_{max}}\right)^2 \tag{35}$$

where K_A and K_B are the Fourier inversion of K_A^* and K_B^*
respectively, i.e.

$$K_A(x,y) = \left(\frac{1}{2\pi}\right)^2 \iint\limits_{-\infty}^{\infty} K_A^* \ e^{\ i(\alpha x + \gamma y)} \ d\alpha d\gamma$$

and $\qquad\qquad\qquad\qquad\qquad\qquad\qquad\qquad\qquad\qquad\qquad$ (36)

$$K_B(x,y) = \left(\frac{1}{2\pi}\right)^2 \iint\limits_{-\infty}^{\infty} K_B^* \ e^{\ i(\alpha x + \gamma y)} \ d\alpha d\gamma$$

K_A is the same as Ventres' K with his uniform thickness replaced by
δ_{max}. The numerical inversion of K_B^* to give K_B is straight forward.
Both K_A and K_B for two dimensional shear flow are shown in Figure 3.
We further assume that

$$\frac{P_W(x,y;\delta(x,y))}{\rho U_1^2} = \frac{P_{W0}(x,y)}{\rho U_1^2} + \left(1 - \frac{\delta(x,y)}{\delta_{max}}\right) \frac{P_{W1}(x,y)}{\rho U_1^2} + 0\left(1-\frac{\delta(x,y)}{\delta_{max}}\right)^2 \tag{37}$$

which is presumably allowed as far as $\delta(x,y)$ is not anywhere near zero.
Substituting Equations (35) and (37) into Equation (29), one can equate
the terms of zeroth and first powers of $\left(1 - \frac{\delta(x,y)}{\delta_{max}}\right)$ to yield the following
two kernel function forms:

$$\frac{W(x,y)}{\bar{U}_1} = \iint\limits_{\substack{\text{wing} \\ \text{surface}}} K_A(x-x', y-y') \frac{p_{W_0}(x',y')}{\rho \bar{U}_1^2} dx'dy' \tag{38}$$

and

$$\frac{W_{eq}(x,y)}{\bar{U}_1} = \iint\limits_{\substack{\text{wing} \\ \text{surface}}} K_A(x-x', y-y') \frac{p_{W_1}(x',y')}{\rho \bar{U}_1^2} dx'dy' \tag{39}$$

where W_{eq} is an equivalent upwash in terms of the lowest order solution $p_{W_0}(x,y)$ i.e.

$$\frac{W_{eq}(x,y)}{\bar{U}_1} = \iint\limits_{\text{Wing area}} -K_B(x-x', y-y') \frac{p_{W_0}(x',y')}{\rho \bar{U}_1^2} dx'dy' \tag{40}$$

The domains of integration of the integrals in Equations (38), (39) and (40) cover only the wing surface area because the pressure is zero everywhere off the wing surface for the lifting surface problem.

Then the solution procedures are

(1) to solve for $p_{W_0}(x,y)$ from Equation (38) for a given upwash $W(x,y)$,

(2) to calculate the equivalent upwash $W_{eq}(x,y)$ from Equation (40),

(3) to solve for $p_{W_1}(x,y)$ from Equation (39), and

(4) to form the final solution using Equation (37).

Thus a lifting surface theory for variable thickness shear flow is completed. It is seen from Equation (37) that the local pressure depends solely on its local boundary layer thickness for a slowly varying boundary flow to the lowest order approximation. However, Equation (29) says that not only the variable $\delta(x,y)$ should be

included in the kernel function K but also the wall pressure appears in the integral equation as the fictitious pressure $P_W(x',y', \delta(x,y))$ which is not the true wall pressure $P_W(x,y; \delta(x,y))$. The latter was not seen from Ventres' uniform thickness solution although the replacement of δ in the kernel function was suggested, and the expansions, equations (33) and (37) are required to render the two integral equations (38) and (39) in conventional kernel function form.

The expansion parameter in the above analysis has been chosen to be $(1 - \frac{\delta}{\delta_{max}})$. An alternate series expansion can be worked out using the parameter $\frac{d\delta}{dx}(\delta = \delta_{max})$. The former expansion involves the detailed boundary layer thickness variation, while the latter *is* only concerned with the trailing edge boundary layer thickness variation. However, P_{W_1} in Equations (22) and (37) remains the same for both choices of the expansion parameter. Although the latter expansion is probably formally preferable since a uniform series convergence is expected, the numerical results shown below have been carried out using the former.

IV. PRESENTATION OF COMPUTATIONAL RESULTS

The shear flow lifting surface theory derived above has been used
to calculate the pressure load on a two dimensional flat plate air-
foil of finite chord in steady shear flow. Both Ventres' uniform
thickness results and the present variable thickness results are
presented for comparison. The familiar collocation method was used.
The pressure was expanded as a linear combination of selected modal
functions and the upwash was matched at all the collocation points
The assumed modal functions, $(x/_c)^n \sqrt{(1-x/_c)/(x/_c)}$ for n = 0, 1, 2,....,
are equivalent to but slightly different from those used by Ventres[19].
The details can be found in his paper and are not elaborated here. Shown
below are (a) the pressure distributions, (b) the total lift coefficients,
and (c) the corresponding center of pressure travel for a turbulent
shear flow model. In addition, a lift coefficent result for a laminar
shear flow model is given. For the turbulent shear flow case, the
boundary layer was assumed to grow according to $\delta(x)/\delta_{max} = (x/_c)^{4/5}$.
For the laminar shear flow case, it is assumed that $\delta(x)/\delta_{max} =$
$(x/_c)^{1/2}$.

(a) Pressure Distributions - Turbulent Boundary Layer

Figures 4 and 5 show typical pressure distributions along the
chord for two different ratios of the trailing edge boundary layer
thickness to the chord length. The exponent N in the velocity
power law is chosen as 7. It is seen that the variable thickness
curve fits in between the potential flow (top curve) and the uniform
shear (lower curve) results. The thicker the boundary layer is,

the larger the shear layer effect is on the pressure load. This
is mainly due to the augmentation of the momentum thickness of
the boundary layer which reduces the momentum transferred to the
perturbed surface. Similar results for the N = 11 case have
been calculated and show less shear effect because the N = 11
case is closer to the potential flow (N = ∞) than N = 7 case
as far as the mean flow velocity distribution is concerned.

(b) Lift Coefficients - Turbulent Boundary Layer

The normalized lift coefficients are plotted in Figures 6
and 7 for N = 7 and N = 11 cases. Figure 6 indicates a 5%
increase in the total lift for the variable δ compared to the
uniform δ case corresponding to δ_{max}/c = .1 and N = 7. Figure
7 shows less change as expected. The reduction of lift coeffici-
ents is a natural result of the pressure decrease due to the
existence of the shear layer.

(c) Center of Pressure Positions - Turbulent Boundary Layer

Figures 8 and 9 demonstrate the shear layer effect on the
center of pressure location. It is seen that the thicker boundary
layers result in further backward movement of the center of
pressure behind the quarter chord. This is caused by the more sig-
nificant pressure reduction near the loading edge than that near
the trailing edge for the shear flow.

(d) Lift Coefficient for A Laminar Boundary Layer Flow

Figure 10 shows the calculated lift coefficient for a
laminar flow. The choice of N= 2.1 simulates the Blasius'
laminar boundary layer velocity profile in an approximate way
as shown in Figure 11. The choice of N = 2.1 instead of N = 2 is

because the kernel function is singular at $N = 2$. Due to this singularity the accuracy of the laminar result is somewhat suspect although Figure 10 shows the same tendency as the turbulent result. For $N = 2$ the present theory simply predicts zero lift. This is because the kernel function tends to infinity everywhere as $N \to 2$ and hence one must have zero wall pressure to balance the finite upwash on the left hand side of the equation (38). This fact points out the limit of validity of the present shear flow model for (nearly) laminar mean flow. Thus, one ought to include the viscosity effect, which is neglected in our shear flow model, in the analysis for the laminar boundary layer or, equivalently, postulate a finite wall velocity according to Lighthill[3].

V.   CONCLUSION

A method of calculating the pressure distribution on lifting surfaces in incompressible shear flows with slowly varying boundary layer thickness has been developed. The assumed mean flow velocity profile, $u/_{U_1} = (z/_\delta (x,y))^{1/N}$, is a good approximation for turbulant boundary layers at high Reynold's numbers, although it predicts an infinite wall shear stress. An interesting point of using this velocity profile is the assumed zero mean flow velocity at the wall which avoids the problem of postulating a finite wall velocity as many authors have done. In any case the boundary layer reduces the pressure load compared to the potential flow, but the variable thickness shear flow model reduces it less for equal maximum shear layer thickness.

The present theory for the variable thickness problem has been worked out in detail for the steady, incompressible case. Its extension to three dimensional, unsteady compressible flows seems to be workable. However, a question does arise as to whether the assumed pressure mode functions for supersonic flows should satisfy the kutta condition at the trailing edge. This is not clear because the flow is subsonic near the solid surface and is supersonic away from the surface.

APPENDIX

STEADY AIRFOIL MOTION IN A SHEAR LAYER OF VARIABLE THICKNESS

We first consider for simplicity two-dimensional flow; it will
be clear that the basic result holds in three-dimensions. Beginning
with the equations of a fully viscous flow (Navier-Stokes equations)[22],

$$\frac{\partial u}{\partial x} + \frac{\partial w}{\partial z} = 0 \qquad \text{continuity} \quad (1)$$

$$u \frac{\partial u}{\partial x} + w \frac{\partial u}{\partial z} = -\left(\frac{1}{\rho}\right) \frac{\partial p}{\partial x} + \nu \left(\frac{\partial^2 u}{\partial x^2} \frac{\partial^2 u}{\partial z^2}\right) \qquad \begin{array}{l} \text{streamwise} \\ x - \text{component of} \\ \text{momentum balance} \ (2) \end{array}$$

$$u \frac{\partial w}{\partial x} + w \frac{\partial w}{\partial z} = -\left(\frac{1}{\rho}\right) \frac{\partial p}{\partial z} + \nu \left(\frac{\partial^2 w}{\partial x^2} + \frac{\partial^2 w}{\partial z^2}\right) \qquad \begin{array}{l} \text{transverse} \\ z - \text{component of} \\ \text{momentum balance} \ (3). \end{array}$$

We now construct an order of magnitude analysis of the various terms.
For this purpose several scale factors are introduced. The boundary
layer thickness, δ , is a characteristic length of the mean (shear)
flow in the z direction; ℓ is a characteristic length in the x direct-
ion associated with the growth of the boundary layer thickness; and a is
a characteristic length in the x direction associated with the variation
of airfoil upwash or angle of attack. First consider the mean flow with no
upwash or angle of attack perturbation. We assume that

$$\frac{\partial}{\partial x} \sim \frac{1}{\ell} \qquad ; \qquad \frac{\partial}{\partial z} \sim \frac{1}{\delta} \qquad\qquad (4)$$

and
$$\frac{\delta}{\ell} \ll 1.$$

From continuity,

$$0 \left(u/_\ell \right) + 0 \left(w/_\ell \right) = 0 \rightarrow w \sim u \, \delta/_\ell \tag{5}$$

From x - momentum,

$$0 \left(\frac{u^2}{\ell} \right) + 0 \left(\frac{wu}{\delta} \right) = - \left(1/_\rho \right) \frac{\partial p}{\partial x} + 0 \left(\frac{\nu u}{\ell^2} \right) + 0 \left(\frac{\nu u}{\delta^2} \right) \tag{6}$$

Using (5), the two terms on the left hand side of (6) are seen to be of the same order. On the right hand side, the second term may be neglected compared to the last and the latter we require to balance with the left hand side

$$0 \left(\frac{u^2}{\ell} \right) \sim 0 \left(\frac{\nu u}{\delta^2} \right)$$

Thus

$$\delta/_\ell \sim 0 \left(\text{Re} \right)^{-1/2} \tag{7}$$

where the Reynolds number is given by

$$\text{Re} \equiv \frac{u\ell}{\nu}$$

From z - momentum,

$$0 \left(\frac{uw}{\ell} \right) + 0 \left(\frac{w^2}{\ell} \right) = - \left(1/_\rho \right) \frac{\partial p}{\partial z} + 0 \left(\frac{\nu w}{\ell^2} \right) + 0 \left(\frac{\nu w}{\delta^2} \right) \tag{8}$$

Using (5) and (7), we conclude from (6) that

$$- \left(1/_\rho\right) \frac{\partial p}{\partial x} \sim 0 \left(\frac{u^2}{\ell}\right)$$

and from (8)

$$- \left(1/_\rho\right) \frac{\partial p}{\partial z} \sim 0 \left(\frac{u^2}{\ell} \frac{\delta}{\ell}\right)$$

Thus

$$\frac{\partial p}{\partial z} << \frac{\partial p}{\partial x}$$

and the mean pressure is essentially constant through the boundary layer.
These results are well-known, of course, and due to Prandtl[22]. We
shall use a similar approach for the perturbation equations where
there is a non-zero upwash or angle of attack.

Let

$$u\,(x,z) = \bar{u}(x,z) + \hat{u}(x,z)$$

$$w\,(x,z) = \bar{w}(x,z) + \hat{w}(x,z) \qquad\qquad (9)$$

$$p\,(x,z) = \bar{p}(x,z) + \hat{p}(x,z)$$

where - denotes mean flow and ^ perturbation. From our previous
analysis we note that $\bar{p}(x,z) = \bar{p}(x)$. Substituting (9) into (1),
(2), (3) and subtracting out the mean flow equations one obtains the
perturbation equations. These are

$$\frac{\partial \hat{u}}{\partial x} + \frac{\partial \hat{w}}{\partial z} = 0 \qquad\qquad\qquad \text{continuity} \qquad (10)$$

$$\bar{u}\,\frac{\partial \hat{u}}{\partial x} + \hat{u}\,\frac{\partial \bar{u}}{\partial x} + \bar{w}\,\frac{\partial \hat{u}}{\partial x} + \hat{w}\,\frac{\partial \bar{u}}{\partial z}$$

$$= -(1/_\rho) \frac{\partial p}{\partial x} + \nu\left(\frac{\partial^2 \hat{u}}{\partial x^2} + \frac{\partial^2 \hat{u}}{\partial z^2}\right)$$

$$\text{x-momentum} \qquad (11)$$

$$\bar{u} \frac{\partial \hat{w}}{\partial x} + \hat{u} \frac{\partial \bar{w}}{\partial x} + \bar{w} \frac{\partial \hat{w}}{\partial z} + \hat{w} \frac{\partial \bar{w}}{\partial z}$$

$$= -\left(1/_\rho\right) \frac{\partial p}{\partial z} + \nu\left(\frac{\partial^2 \hat{w}}{\partial x^2} + \frac{\partial^2 \hat{w}}{\partial x^2}\right)$$

$$\text{z-momentum} \qquad (12)$$

We assume that

$$\frac{\partial(\ )}{\partial z} \sim (\ )/_\delta \quad ; \quad \frac{\partial(\hat{\ })}{\partial x} \sim (\hat{\ })/_a \quad ; \quad \frac{\partial \bar{(\ )}}{\partial x} \sim \bar{(\ )}/_\ell$$

and $\delta << \ell$

$$\delta/_a \sim 0 (1) \qquad\qquad (13)$$

      $a << \ell$

Other interesting cases could be considered; for example, $\delta/_a >> 1$

or $<< 1$. However, we shall not pursue these here.

From continuity,

$$0 \quad \left(\frac{\hat{u}}{a}\right) + 0 \quad \left(\frac{\hat{w}}{\delta}\right) = 0 \rightarrow \hat{w} \sim \hat{u} \, \delta/_a \qquad (14)$$

From x - momentum,

$$0 \left(\frac{\bar{u}\hat{u}}{a}\right) + 0 \left(\frac{\hat{u}\bar{u}}{\ell}\right)^{\nearrow} + 0 \left(\frac{\bar{u}\delta\hat{u}}{\ell a}\right)^{\nearrow} + 0 \left(\frac{\hat{u}\delta\bar{u}}{a\delta}\right)$$

$$= -(1/_\rho) \frac{\partial p}{\partial x} + 0 \left(\frac{\nu\hat{u}}{a^2}\right) + 0 \left(\frac{\nu\hat{u}}{\delta^2}\right) \qquad (15)$$

In the above, we have used (5) and (14) to replace $\bar{w}$, θ and indicated by an arrow negligibly small terms. By the assumption of $\delta/_{a} \sim O(1)$, the last two terms on the RHS of (15) are of the same order. Let us compare the latter of these to the (remaining) terms on the LHS. Recall from (7) that

$$\frac{\nu}{\bar{u}\ell} \sim (\delta/_\ell)^2$$

Thus

$$\frac{\nu\Omega}{\delta^2} \sim \frac{\bar{u}\Omega}{\ell}$$

which is negligible compared to LHS of (15). Hence, x-momentum equation simplifies to

$$\bar{u} \frac{\partial\Omega}{\partial x} + \theta \frac{\partial\bar{u}}{\partial z} = - (1/_\rho) \frac{\partial\rho}{\partial x} \tag{16}$$

Note that if $a \sim \ell$, then one must include viscous terms and hence the basic validity of a shear flow, as opposed to a fully viscous model is dependent upon $a \ll \ell$. Formally this need not be true for turbulent flow where [22]

$$\frac{\nu}{\bar{u}\ell} \sim (\delta/_\ell)^5$$

However, then the question arises as to what viscosity coefficient one should use[8].

From z-momentum,

$$0 \left(\bar{u} \frac{\hat{u}}{a} \frac{\delta}{a} \right) + 0 \left(\hat{u} \frac{\bar{u}}{\ell} \frac{\delta}{\ell} \right) + 0 \left(\bar{u} \frac{\hat{u}}{a} \frac{\delta}{\ell} \right)$$

$$+ 0 \left(\hat{u} \frac{\bar{u}}{a} \frac{\delta}{\ell} \right) = - (1/\rho) \frac{\partial \hat{p}}{\partial z} + 0 \left(\bar{u} \frac{\hat{u}}{\ell} \frac{\delta}{a} \right) \tag{17}$$

where we have used (5), (7) and (14) to simplify terms in (17) and indicated by an arrow those which are negligibly small. Thus the z-momentum equation becomes

$$\bar{u} \frac{\partial \hat{w}}{\partial x} = - (1/\rho) \frac{\partial \hat{p}}{\partial z} \tag{18}$$

Our final equations are then (10), (16) and (18). Using these we may obtain a single equation for p,

$$\nabla^2 p - 2 \frac{\frac{\partial U}{\partial z}}{U} \frac{\partial p}{\partial z} - \frac{\partial p}{\partial x} \frac{\frac{\partial U}{\partial x}}{U} = 0 \tag{19}$$

where the last term may be neglected consistent with our previously announced assumptions on the various length scales. Note that we have dropped the ^ and replaced $\bar{u}$ by U.

REFERENCES

1. Tsien, H. S., "Symmetrical Joukowsky Airfoils in Shear Flow", Quarterly of Applied Mathematics, Vol.1, No. 1, April 1943, pp.130-148.

2. Von Kármán, Th. and Tsien, H. S., "Lifting Line Theory of a Wing in Non-uniform Flow", Quarterly of Applied Mathematics, Vol.3, No.1, April 1945, pp. 1-11.

3. Lighthill, M. J., "On Boundary Layers and Upstream Influence II. Supersonic Flows without Separation", Proceedings of the Royal Society, Series A, Vol. 217, No. A 1131, May 1953, pp. 478-507.

4. Lighthill, M.J., "The Fundamental Solution for Small Steady Three-Dimensional Disturbances to a Two-Dimensional Parallel Shear Flow", Journal of Fluid Mechanics, Vol.3, Part 2, Nov. 1957, pp. 113-144.

5. Miles, J. W., "On the Generation of Surface Waves by Shear Flows", Vol.3, Part 2, November 1957, pp. 185-204.

6. Miles, J. W., "On Panel Flutter in the Presence of a Boundary Layer", Journal of the Aeronautical Sciences, Vol.26, No.2, Feb. 1959, pp. 81-93.

7. Benjamin, T. B., "Shearing Flow Over a Wavy Boundary", Journal of Fluid Mechanics, Vol.6, Pt. 2, pp. 161-205, 1959.

8. McClure, J. D., "On Perturbed Boundary Layer Flows", M.I.T. Fluid Dynamics Laboratory Report No. 62-2, June 1962.

9. Anderson, W. J. and Fung, F. C., "The Effect of an Idealized Boundary Layer on the Flutter of Cylindrical Shells in Supersonic Flow", SM 62-49, CIT, Pasadena, California 1962.

10. Olsen, M. D., "On Comparing Theory and Experiment for the Supersonic Flutter of Circular Cylindrical Shells", AFOSR 66-0944, Graduate Aeronautical Laboratory, California Institute of Technology, Pasadena, California, June 1966.

11. Zeydel, E. F. E., "Study of the Pressure Distribution on Oscillating Panels in Low Supersonic Flow with Turbulent Boundary Layer", NASA CR-691, February 1967, GIT.

12. Dowell, E. H., "Generalized Aerodynamic Forces on a Flexible Plate Undergoing Transient Motion in a Shear Flow with an Application to Panel Flutter", AIAA Journal, Vol.9, No.5, May 1971, pp.834-841.

13. Ventres, C. S., "Transient Panel Motion in a Shear Flow", AMS Report 1062, August 1972, Princeton University, Princeton, N.J.

14. Lerner, J. E., "Unsteady Viscous Effects in the Flow Over an Oscillating Surface", SUDAAR Report No.453, Stanford University, December 1972.

15. Eversman, W. and Beckemeyer, R. J., "Transmission of Sound in Ducts with Thin Shear Layers-Convergence to the Uniform Flow Case", Journal of the Acoustical Society of America, Vol.52, No.1, July 1972, pp. 216-220.

16. Dowell, E. H. and Ventres, C. S., "Derivation of Aerodynamic Kernel Functions", AIAA Journal, Vol.11, No.11, November 1973, pp. 1586-1588.

17. Yates, J. E., "Linearized Integral Theory of Three-Dimensional Unsteady Flow in a Shear Layer", AIAA Journal, Vol.12, No.5, May 1974, pp. 596-601.

18. Beckemeyer, R. J., "Application of an Inner Expansion Method to Plane, Inviscid, Compressible Flow Stability Studies", Journal of Fluid Mechanics, Vol.62, Part 2, January 1974, pp. 405-416.

19. Ventres, C. S., "Shear Flow Aerodynamics: Lifting Surface Theory", to be published in AIAA Journal.

20. Ludwig, G. R., and Erickson, J. C., Jr., "Airfoils in Two dimensional Non-Uniformly Sheared Slip-Stream", Journal of Aircraft, Vol.8, No.11, November 1971, pp. 874-884.

21. Nayfeh, A. H., "Perturbation Methods", Wiley-Interscience, 1973, Chapter 6.

22. Schlichting,H., "Boundary-Layer Theory", Sixth Edition, McGraw-Hill Book Company, 1968, Chapters 3 and 21.

FIG. 1

$$\frac{U}{U_1} = \left(\frac{z}{\delta}\right)^{1/N}$$

$$\delta K = \frac{\delta}{\pi x} \quad \text{FOR } N = \infty$$

$$\delta K \rightarrow \frac{\delta}{\pi x} \quad \text{FOR } \frac{x}{\delta} \rightarrow \infty$$

FOR ANY N
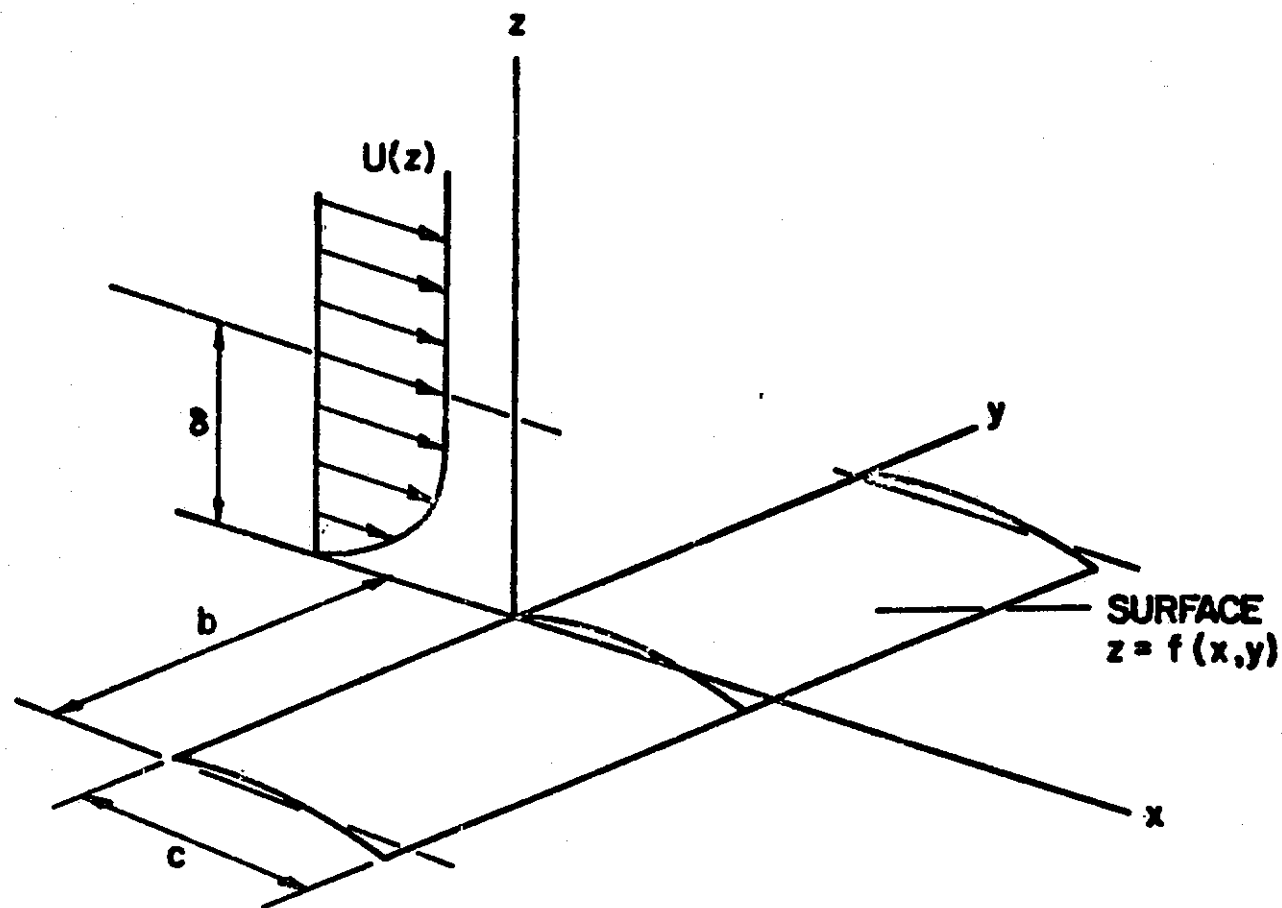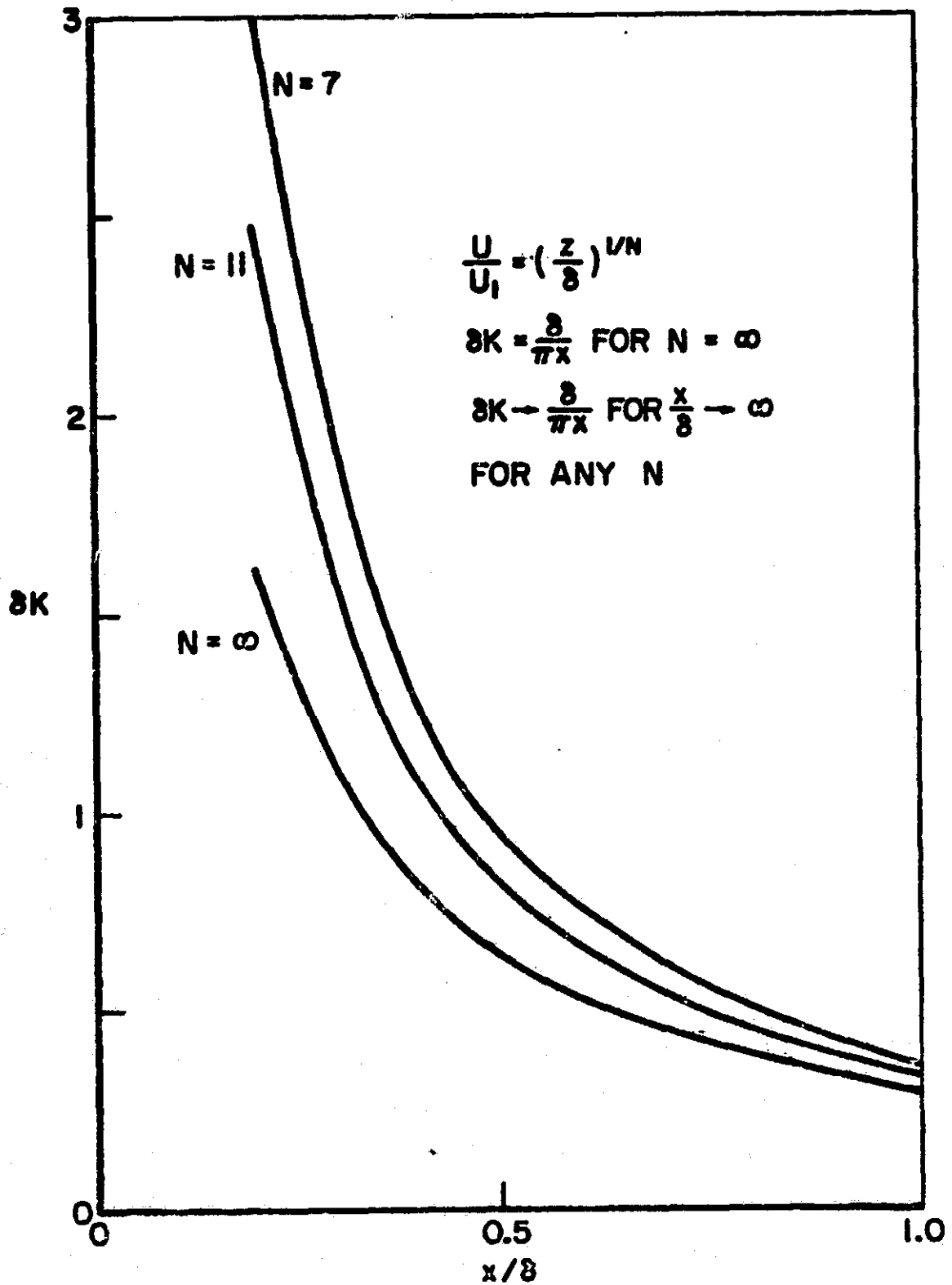
FIG. 2 · KERNEL FUNCTION

FIG. 3 : KERNEL FUNCTIONS

N = 7

$$\delta_{max} K_B = \delta_{max} K_B' - \frac{2}{N} \delta_{max} K_A$$

$\delta_{max} K_A$

$\delta_{max} K_B'$

ZERO CROSSING BETWEEN X/δ_{max} = 3 AND 4

$\delta_{max} K_B$

X/δ_{max}
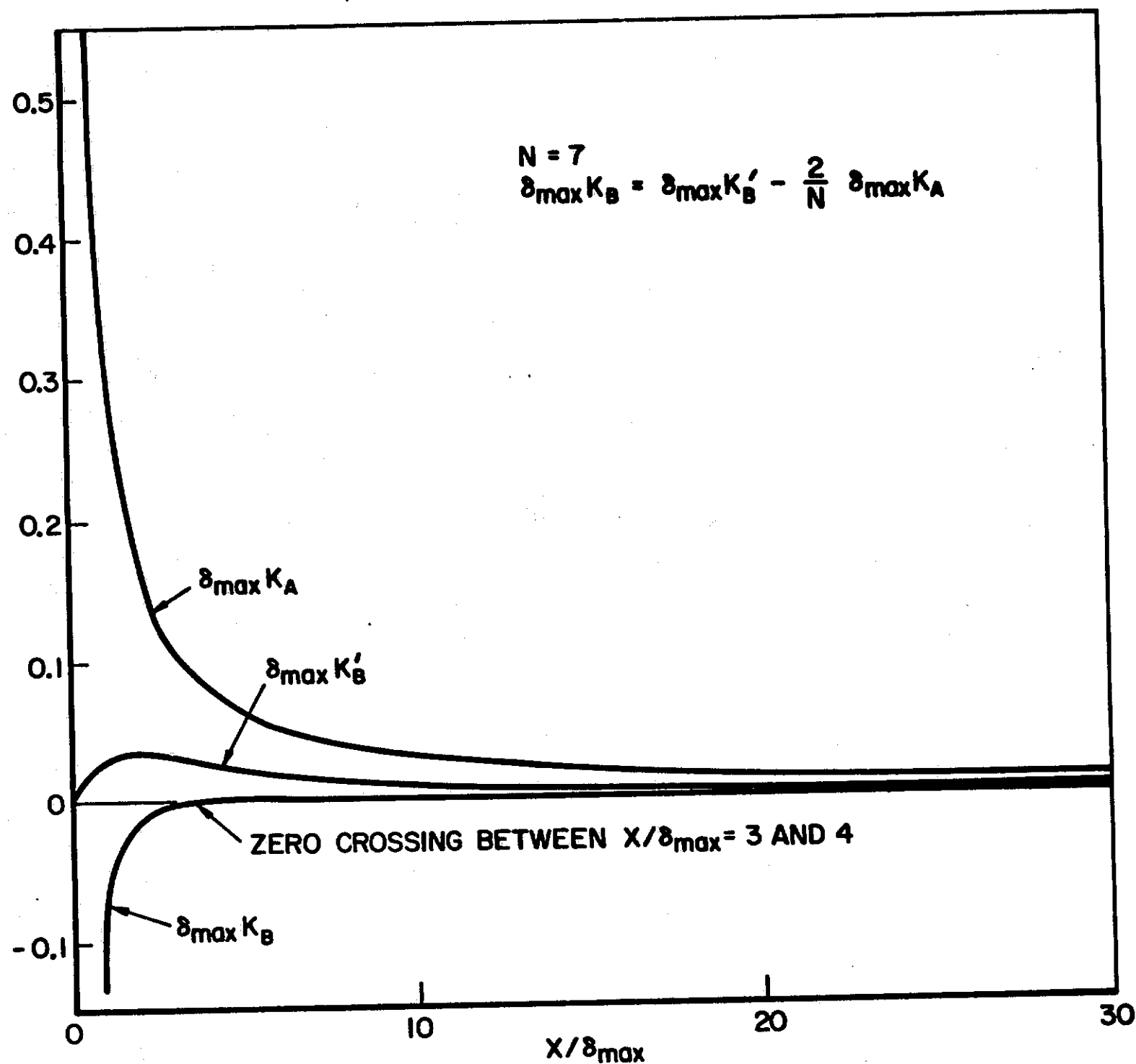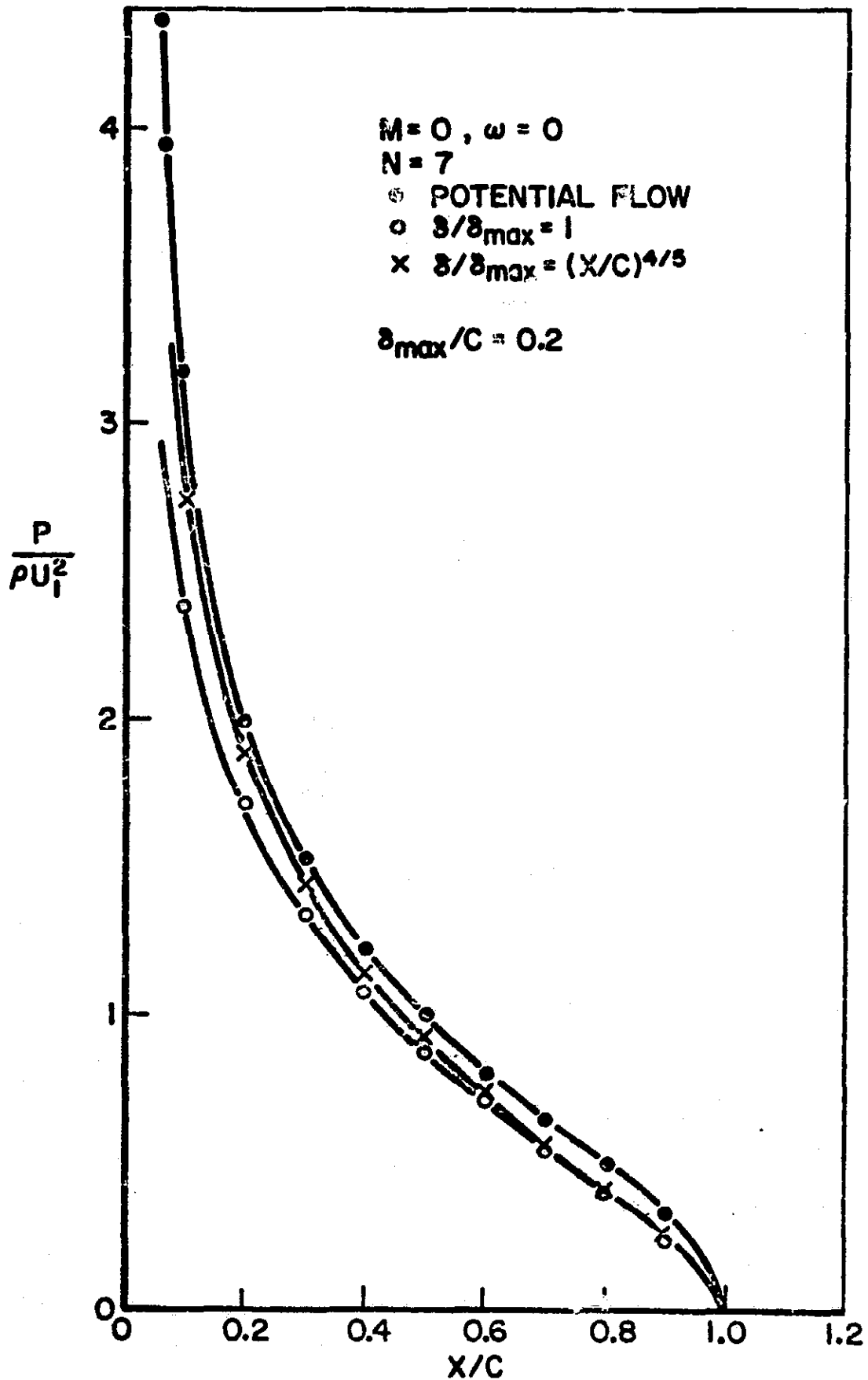
FIG. 4 · PRESSURE DISTRIBUTION ALONG CHORD
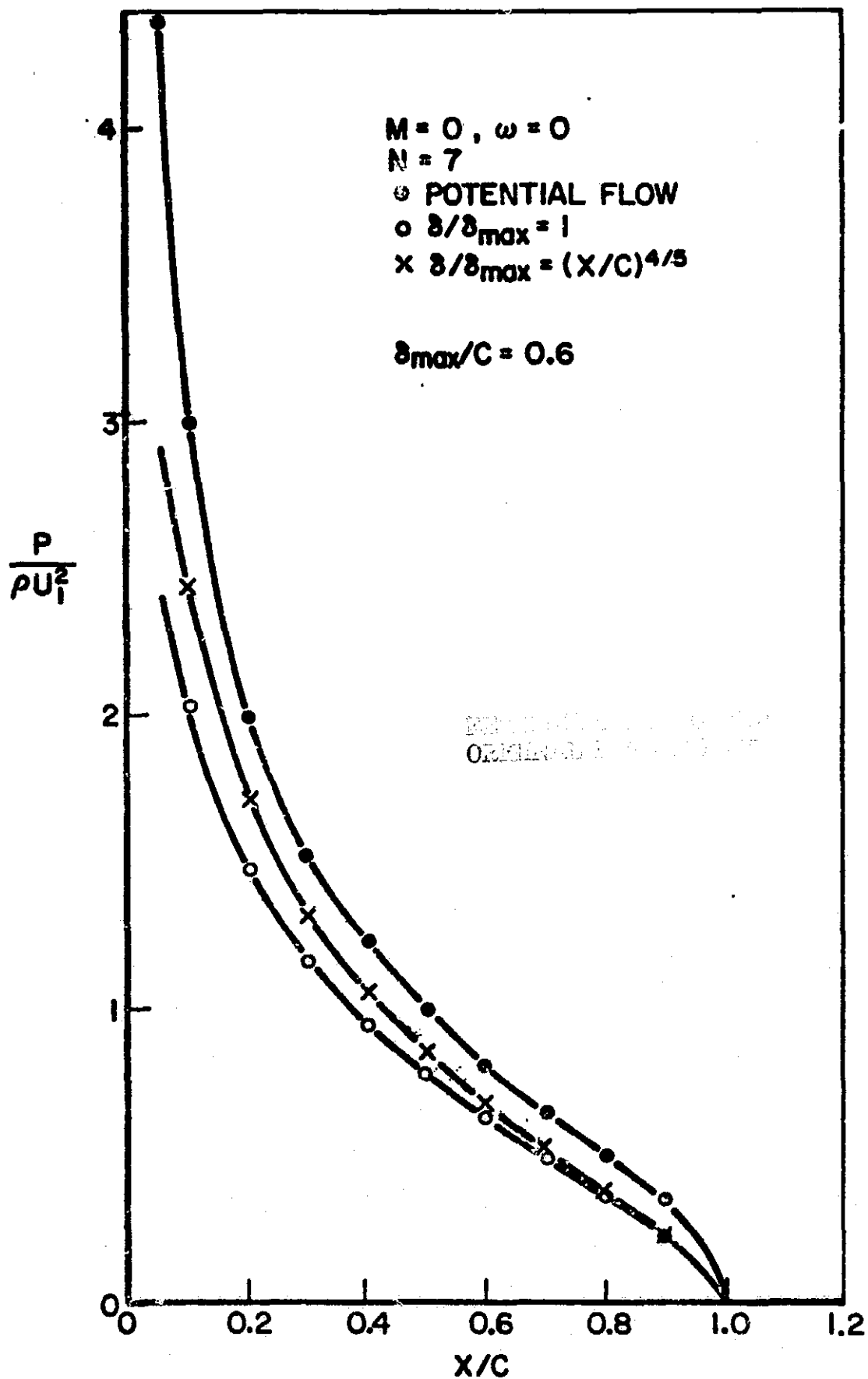
FIG. 5 · PRESSURE DISTRIBUTION ALONG CHORD
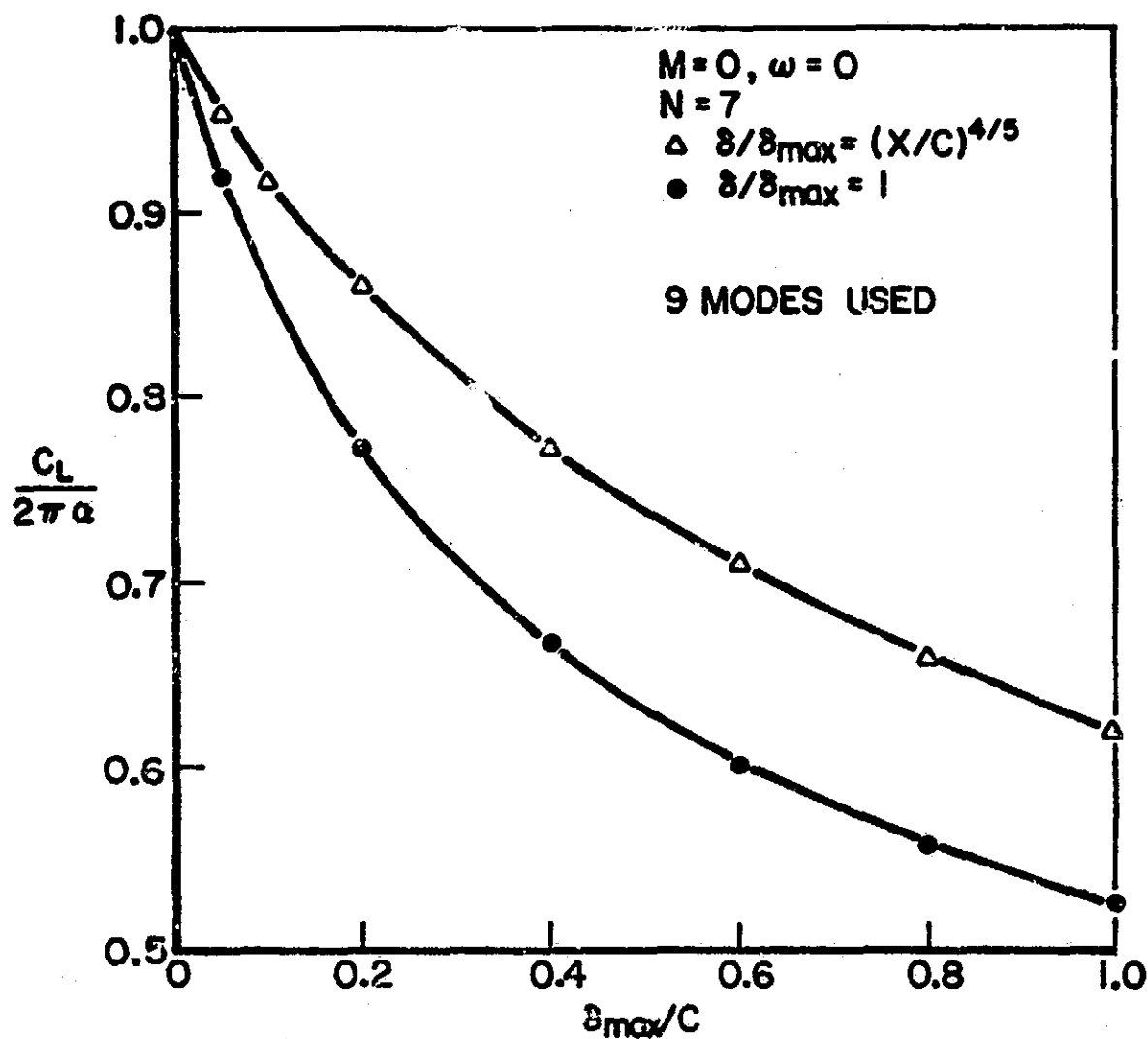
FIG. 6· LIFT COEFFIENT vs δ_{max}/C FOR BOTH UNIFORM AND VARIABLE BOUNDARY LAYER THICKNESS OF THE CASE N = 7
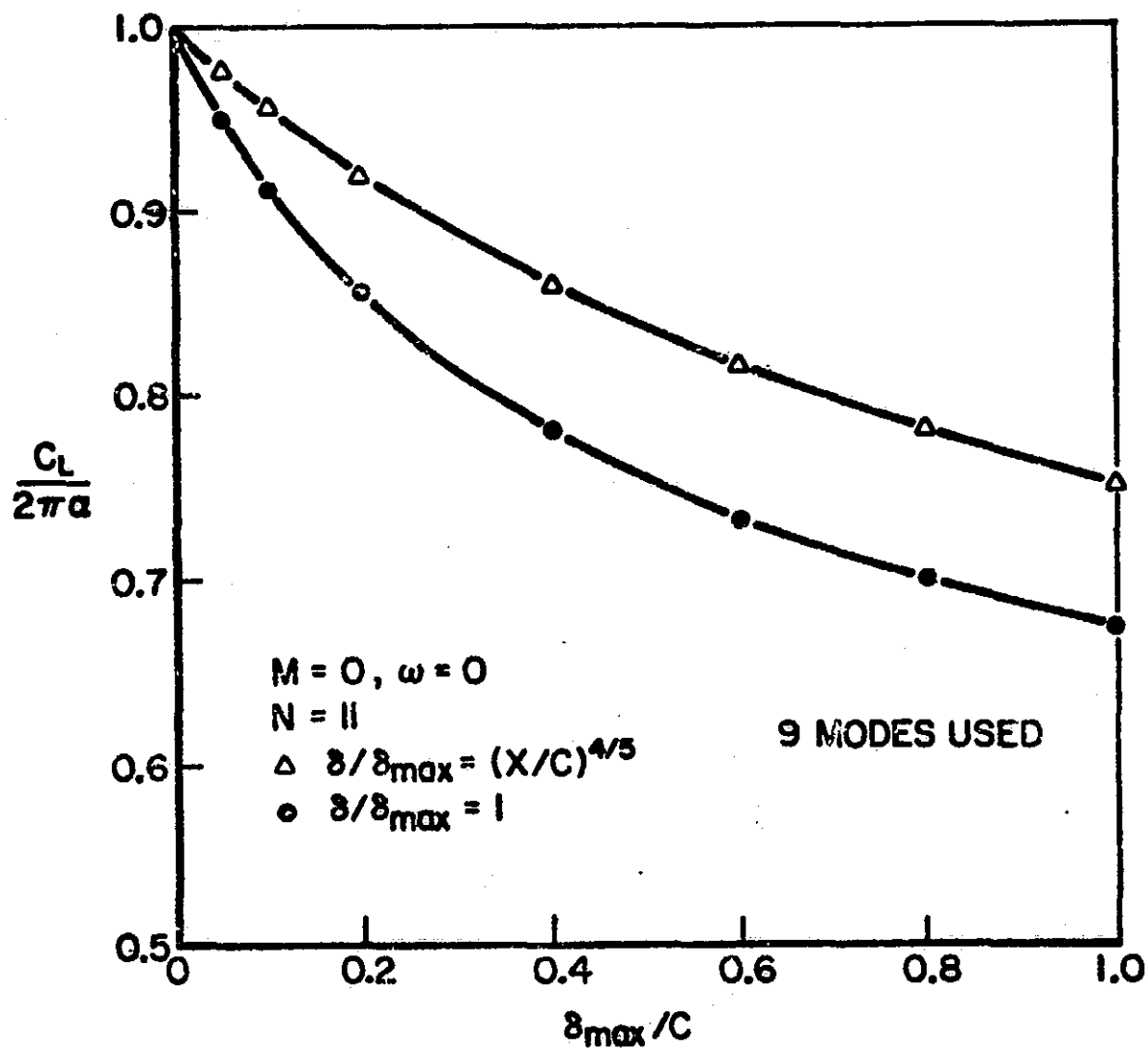
FIG. 7 · LIFT COEFFICIENT vs δ_{max}/C FOR BOTH UNIFORM AND VARIABLE BOUNDARY LAYER THICKNESS OF THE CASE N = II
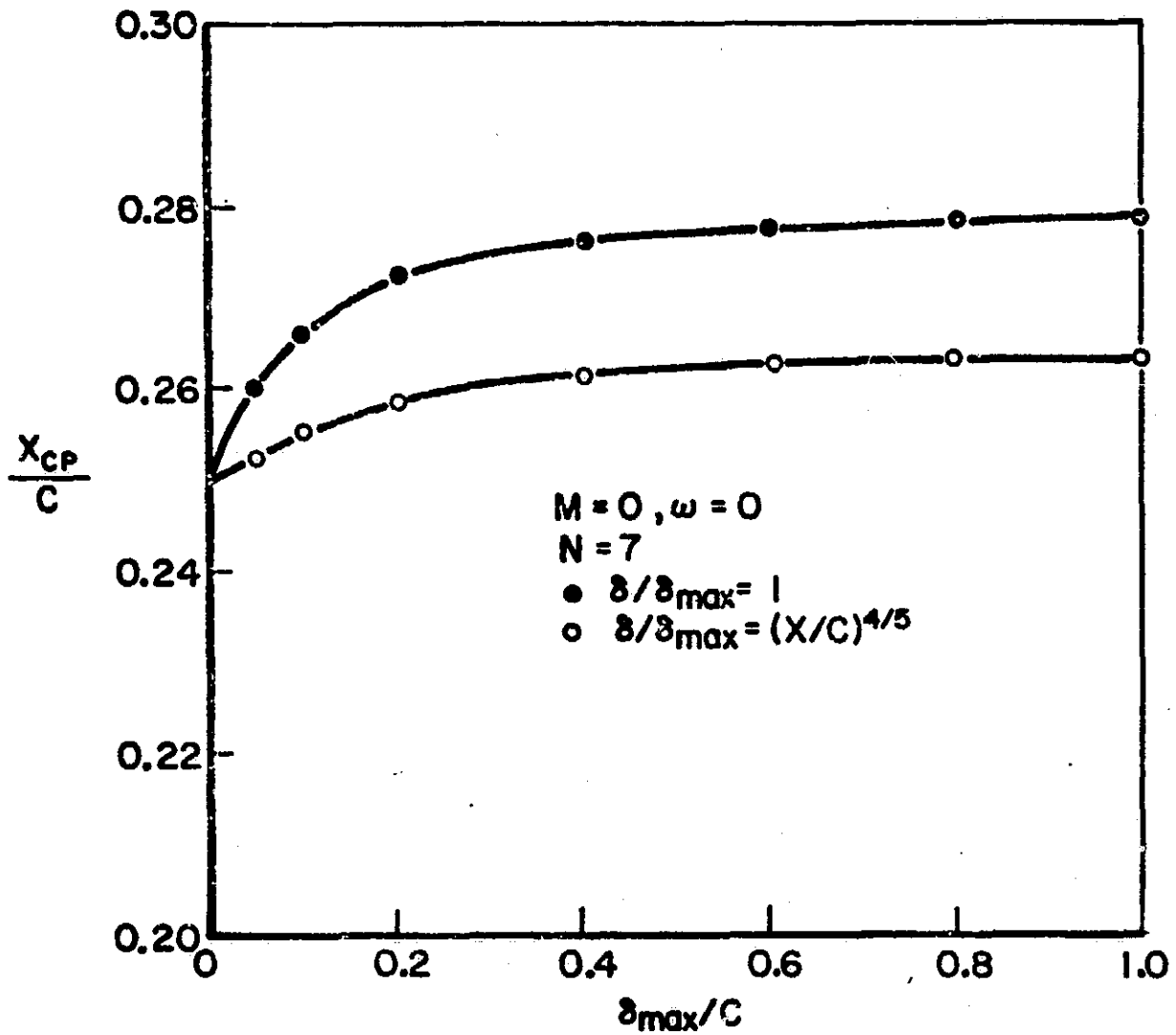
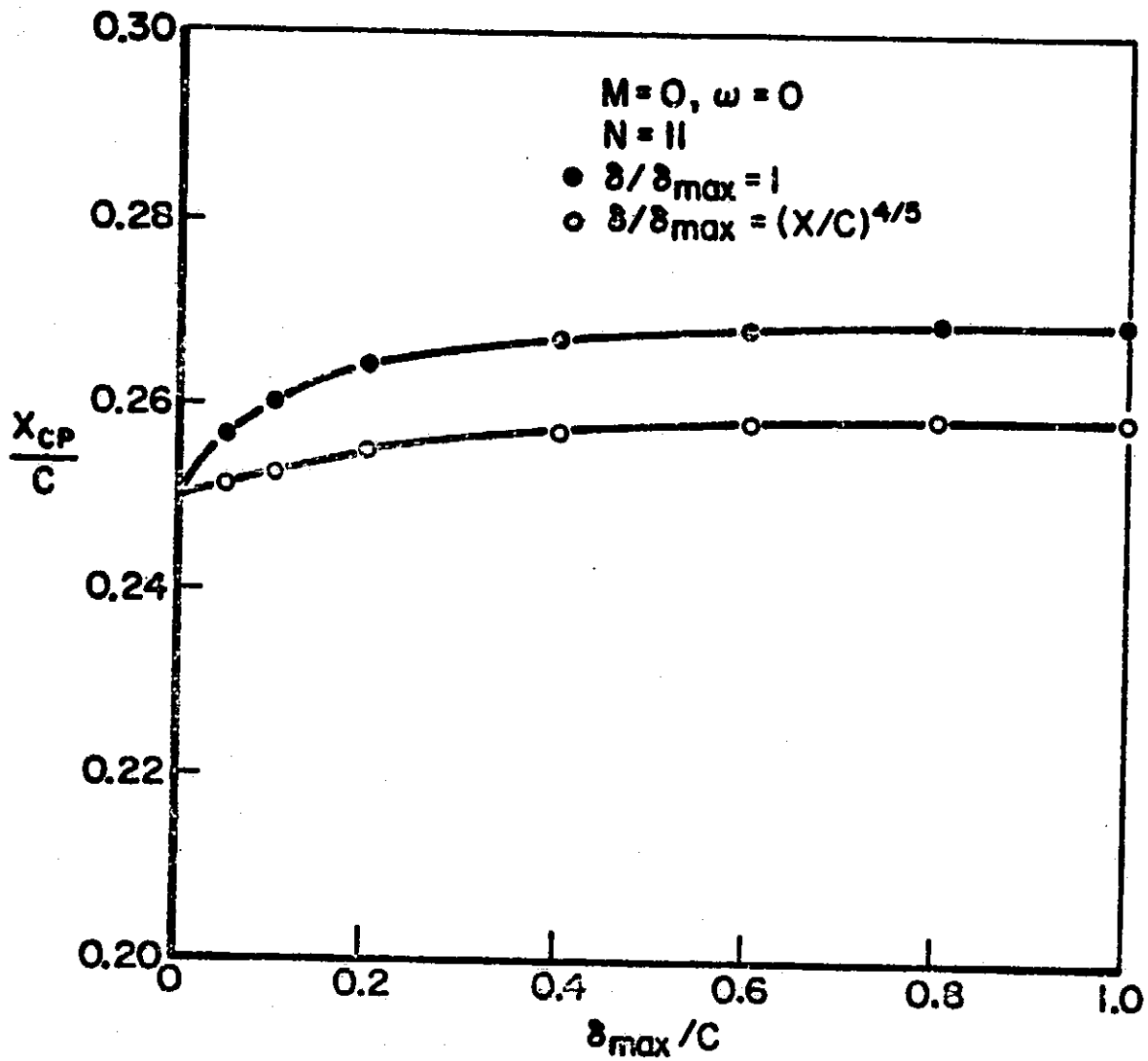FIG. 8· POSITION OF CENTER OF PRESSURE vs δ_{max}/C FOR THE CASE N = 7

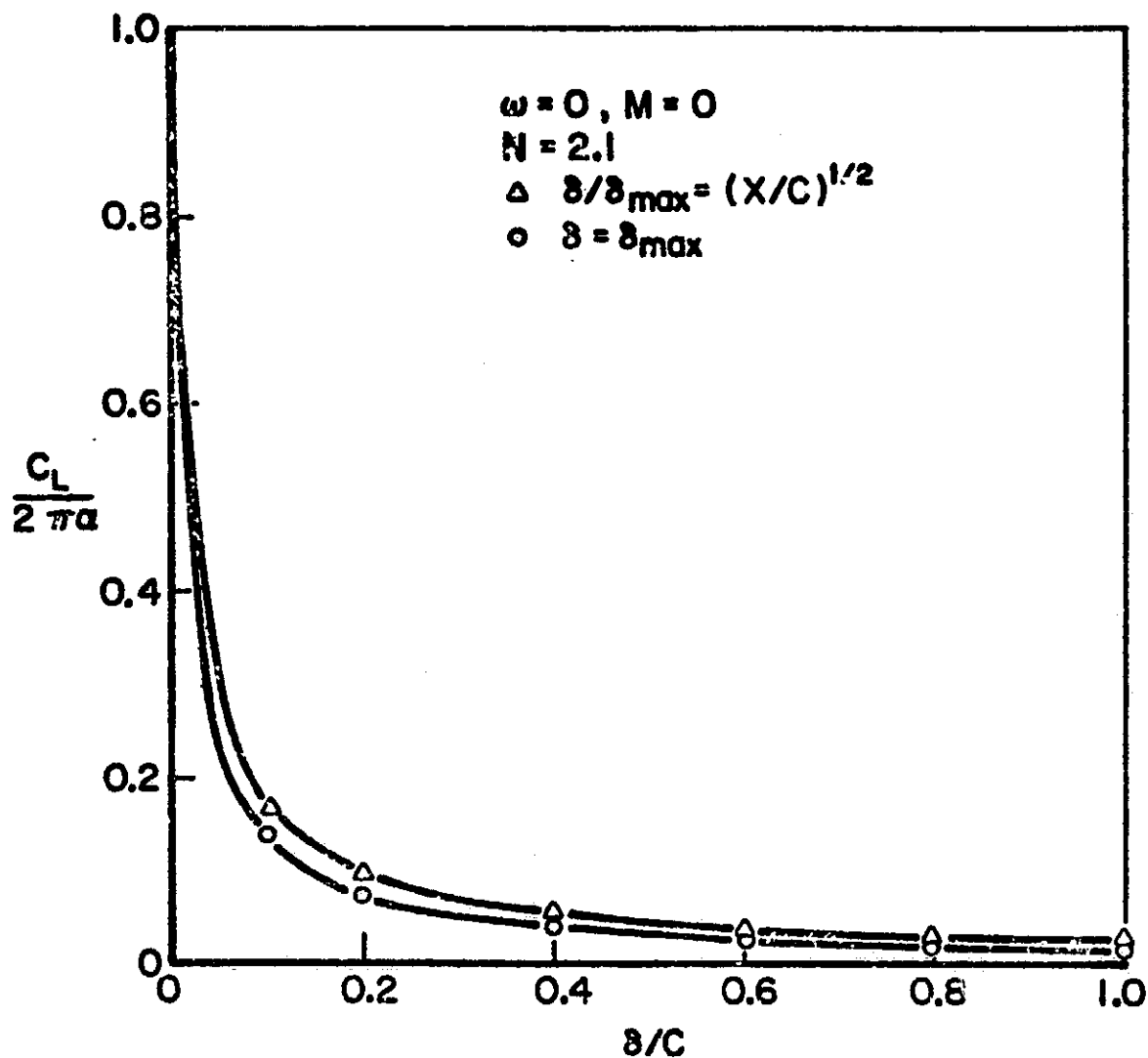FIG. 9· POSITION OF CENTER OF PRESSURE vs δ_{max}/C FOR THE CASE N = 11

FIG. 10 · LIFT COEFFICIENT vs δ_{max}/C FOR BOTH UNIFORM AND VARIABLE BOUNDARY LAYER THICKNESS OF THE CASE N = 2.1
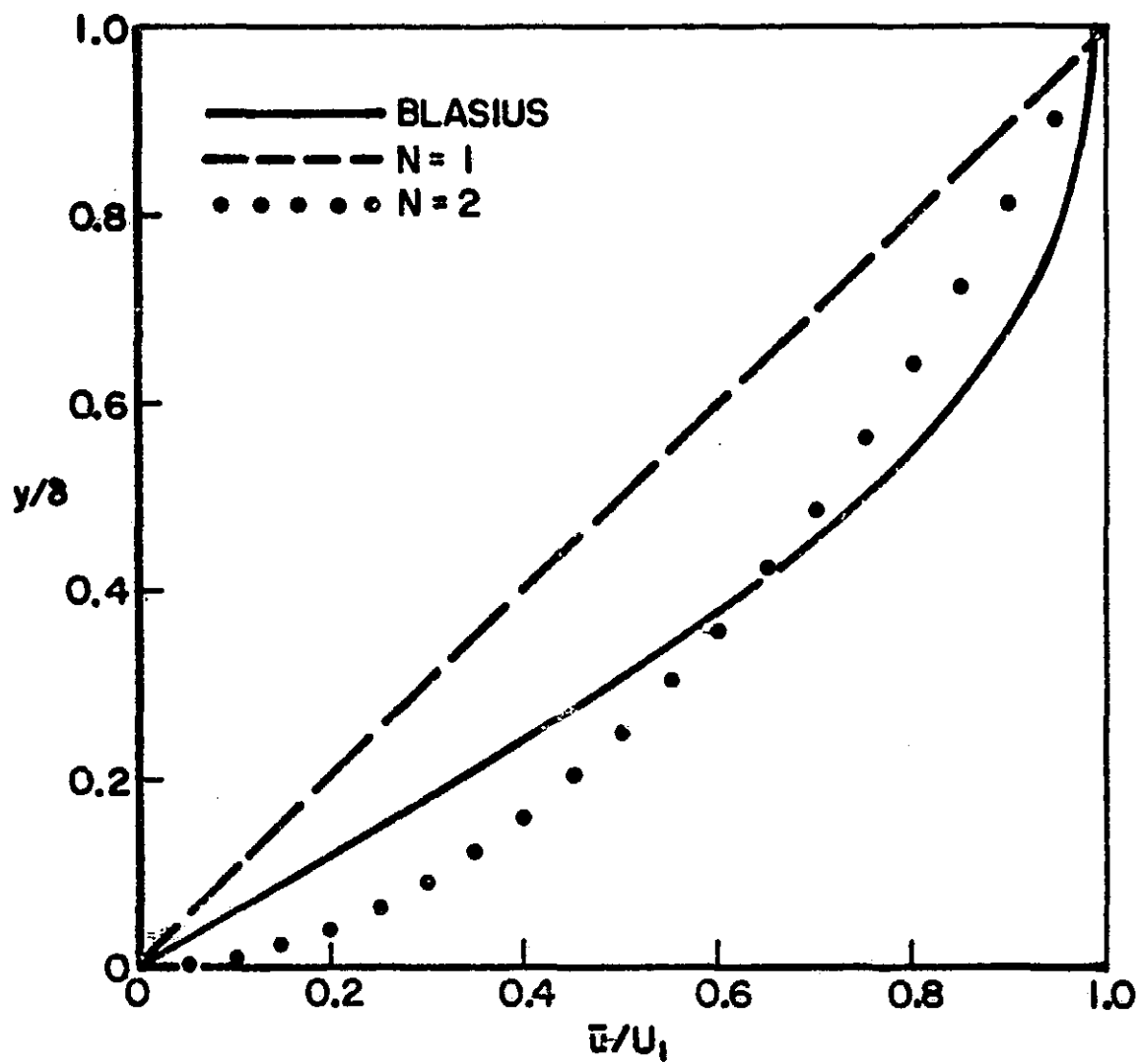
FIG. II · LAMINAR BOUNDARY LAYER VELOCITY PROFILE